PHYSICAL REVIEW E **84**, 061142 (2011)

Statistical thermodynamics of straight rigid rods with nonadditive lateral interactions: Theory and Monte Carlo simulations

O. A. Pinto, F. Nieto, and A. J. Ramirez-Pastor[*]

Departamento de Física, Instituto de Física Aplicada, Universidad Nacional de San Luis-CONICET,
Chacabuco 917, 5700 San Luis, Argentina

(Received 19 August 2011; revised manuscript received 29 November 2011; published 27 December 2011)

The statistical thermodynamics of straight rigid rods of length k (k-mers) with nonadditive lateral interactions was developed on a generalization in the spirit of the lattice-gas model and the classical Bragg-Williams approximation (BWA) and the quasichemical approximation (QCA). The new theoretical framework is obtained by combining (i) the exact analytical expression for the partition function of noninteracting linear k-mers adsorbed in one dimension and its extension to higher dimensions, and (ii) a generalization of BWA and QCA in which the adsorbate can occupy more than one adsorption site. The traditional assumption of a strictly pairwise additive nearest-neighbors interaction is replaced by a more general one, namely that the bond linking a certain atom with any of its neighbors depends considerably on how many of them are actually present (or absent) on the sites in the first coordination shell of the atom. The coverage and temperature dependence of the Helmholtz free energy, chemical potential, configurational entropy, and differential heat of adsorption are given. The formalism (i) reproduces the classical results for monomers, (ii) leads to the exact statistical thermodynamics of nonadditive interacting k-mers adsorbed in one dimension, and (iii) provides a close approximation for two-dimensional systems, taking into account multisite occupancy and nonadditive lateral interactions. Comparisons with Monte Carlo simulations are performed in order to test the validity of the theoretical model. Significant quantitative differences are shown and discussed. In all cases, the QCA appears to be the more accurate approach.

DOI: 10.1103/PhysRevE.84.061142 PACS number(s): 05.50.+q, 68.43.−h, 05.10.Ln

I. INTRODUCTION

The adsorption of gases on solid surfaces is a topic of fundamental interest for various applications [1,2]. From the theoretical point of view, the process can be described in terms of the lattice-gas model [3–8]. The lattice-gas model is characterized by a division of the volume [or area in the two-dimensional (2D) case] into cells such that the number of cells is larger than the number of particles. Each cell is centered at one site of a lattice. For the interaction energy, the following assumption is made: the potential energy between two particles is $+\infty$ if they are in the same cell, w if they are in a pair of neighboring cells, and zero otherwise.

Over the years, numerous generalizations of the standard lattice-gas theory have been proposed to describe chemisorbed or physisorbed monolayers at crystalline surfaces [9–11]. However, in all cases, the models preserve a fundamental statistical property, the well-known symmetry particle vacancy [12].

For several experimental arrangements, the behavior of the thermodynamic quantities and the phase diagram of the system have shown clear signals of the nonequivalence between particles and vacancies. In fact, adsorption isotherms for methane, ethane, and others adsorbed on $AlPO_4$-5 and SAPO-5 are clearly unsymmetrical around half-coverage [13–17]. These phenomena are also visible in the isosteric heat of adsorption. Surface restructuring is another example of a system that differs significantly from that which can be predicted by using a standard lattice-gas model.

The two main routes to break the symmetry particle vacancy are the following: (i) to introduce some sort of local correlation, such as particles that occupy several k contiguous lattice sites; and (ii) to consider nonpairwise (nonadditive) lateral interactions between the adsorbed molecules. The properties (i) and (ii) have been recognized in several experimental systems. In fact, even the simplest nonspherical molecules such as N_2, O_2, and CO may adsorb on more than one site depending on the surface structure [18–21]. Larger linear molecules such as $C_nH_{2(n-1)}$ (n-alkanes) adsorbed on solid surfaces should be regarded under the light of a multisite adsorption model [22–24] in order to properly account for the effects of configurational entropy (adsorbate size and flexibility) on the thermodynamics of the adlayer.

On the other hand, nonadditive ad-ad interactions have been observed in several experimental systems: H on Pd(100) [25], O on W(110) [26], H on Fe(110) [27], and the Ga-Pb alloy [28], just to name a few. In addition, the presence of nonadditivity in the interactions has been observed in the study of monolayer growth in a heteroepitaxial system with the presence of heterogeneities [Ag/Au(100), Ag/Pt(100), Au/Pt(100), Au/Pd(100), Au/Ag(100), Pt/Ag(100), Pt/Au(100), and Pd/Au(100)] [29–31] and in the electrochemical phase formation [Ag on Au(111) and Au(100)] [32–34].

From a theoretical point of view, the consequences of considering nonadditive interactions in the adsorption thermodynamics have been studied for a long time. In fact, statistical mechanics of adsorbed monolayers has been the subject of analytical treatment by means of the Bragg-Williams approximation (BWA) [35–37], the quasichemical approximation (QCA) [38], and Monte Carlo simulations [39–41]. In all cases, one fundamental feature is preserved. This is the assumption that an adsorbed molecule occupies one adsorption site.

In summary, despite over three decades of intensive work, there exists a lack of systematic studies of adsorption systems

---

[*] antorami@unsl.edu.ar.

in the presence of both nonadditive lateral interactions and multisite occupancy. The objective of this paper is to provide a thorough study in this direction. For this purpose, a new theoretical formalism is presented based upon (i) the exact analytical expression for the partition function of noninteracting straight rigid rods of length (k-mers) adsorbed in one dimension and its extension to higher dimensions; [42] and (ii) a generalization of the classical BWA and QCA [12,43], in which the lateral interactions are nonadditive and the adsorbate can occupy more than one adsorption site. In addition, Monte Carlo (MC) simulations are performed in order to test the validity of the theoretical model. The new theoretical scheme allows us (i) to identify and characterize the most prominent features of the effect of the nonadditive interactions on the adsorption thermodynamics of straight rigid molecules; (ii) to develop an improved approximation for two-dimensional adlayers, taking into account multisite occupancy and nonadditive interactions; and (iii) to provide a simple model from which experiments may be reinterpreted.

The paper is organized as follows: In Sec. II, the lattice-gas model for nonadditive interacting rods is presented. In addition, the basis of the Monte Carlo simulation scheme in the grand-canonical ensemble is given. In Sec. III, the analytical form of the main adsorption thermodynamic functions (adsorption isotherm, configurational entropy, and differential heat of adsorption) is derived from the BWA and the QCA. The results of the theoretical approaches are presented in Sec. IV, along with a comparison with Monte Carlo simulation data corresponding to interacting dimers adsorbed on one-dimensional and square lattices. Finally, the conclusions are drawn in Sec. V.

II. BASIC DEFINITIONS: ADSORPTION MODEL AND MONTE CARLO SIMULATION

A. Model

Here, we address the general case of adsorbates assumed to be straight rigid rods containing k identical units, each one occupying a site on a lattice of $M = L \times L$ sites and connectivity γ. Small adsorbates with spherical symmetry would correspond to the monomers limit ($k = 1$). The distance between k-mer units is assumed in registry with the lattice constant a; hence exactly k sites are occupied by a k-mer when adsorbed. Under these considerations, the Hamiltonian of the system can be written as

$$H = \frac{1}{2} \sum_{i,j=1;\, i\neq j}^{M} (W_{i,j}\, c_i\, c_j\, f_{i,j}) + U_0 \sum_{i}^{M} c_i, \qquad (1)$$

where c_i is the occupation variable, which can take the following values: $c_i = 0$ if the corresponding adsorption site i is empty and $c_i = 1$ if the site is occupied; $f_{i,j}$ is defined to take either the value 0 if the sites i and j are occupied by units belonging to the same k-mer or 1 if the sites i and j are occupied by units belonging to different k-mers[1]; U_0 is the constant interaction energy between a k-mer unit and an adsorption site (in the simulations, U_0 is set equal to zero without any lost of generality); and $W_{i,j}$ is the nonadditive lateral interaction energy, which is assumed to have different values, W_m ($m = 1,2,\dots,\lambda$),[2] depending on the number m of occupied first neighbors around a given k-mer. An example illustrating how to obtain the total lateral interaction energy corresponding to a configuration of adsorbed dimers is shown in Fig. 1.

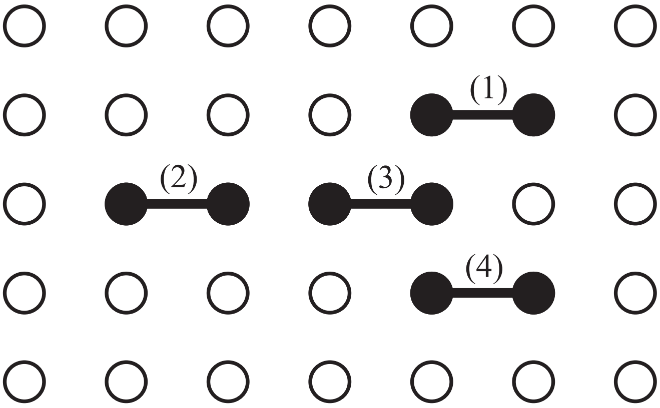

FIG. 1. Snapshot corresponding to a given configuration of dimers adsorbed on a square lattice. Solid circles (joined by thick lines) and empty circles represent dimers and empty sites, respectively. In this case, $m = 1$ for the dimer 1, $m = 1$ for the dimer 2, $m = 3$ for the dimer 3, and $m = 1$ for the dimer 4. Accordingly, the total lateral interaction energy of the configuration is equal to $\frac{1}{2}(W_1 + W_1 + 3W_3 + W_1)$.

As mentioned above, W_m depends on the occupation state of the surrounding of a given k-mer. This dependence is usually not known and is expected to be different in specific cases. Then, we consider the simplest model of nonadditive interaction, where W_m varies linearly with m [37,39],

$$\frac{W_m}{W} = \frac{P\lambda - 1}{\lambda - 1} - m\frac{P - 1}{\lambda - 1}. \qquad (2)$$

In the preceding equation, $W_\lambda = W$ and $P = W_1/W$ is the nonadditivity parameter, which represents the ratio of the strongest to the weakest bonds possible in the system.

As can be observed from Eq. (2), when $P = 1.0$ the problem reduces to the additive form, ($W_1 = W_2 = \cdots = W_\lambda$). For $P < 1.0$ ($P > 1.0$), each interaction is weaker (stronger) than in the additive case. Then, P emerges as an important control parameter for describing the problem.

B. Monte Carlo simulation of adsorption in the grand-canonical ensemble

The problem has been studied by grand-canonical MC simulations using a typical adsorption-desorption algorithm [44]. The system chosen was a lattice gas of interacting dimers (the dimer is the simplest case of a straight rigid rod and contains all the properties of the multisite-occupancy adsorption).

---

[1] Because the present model assumes straight rigid adsorbates, intramolecular interactions (interactions of pairs of units belonging to the same molecules) are not included in Eq. (1).

[2] $\lambda = [2(\gamma - 1) + (k - 2)(\gamma - 2)]$ represents the number of NN sites of an adsorbed k-mer.

The simulation procedure is as follows. For a given value of temperature T and chemical potential μ, an initial configuration with N dimers adsorbed at random positions (on $2N$ sites) is generated. Then, an adsorption-desorption process is started, where a pair of NN sites is randomly chosen and a random number $\xi \in [0,1]$ is generated:

(i) If the two sites are empty, then adsorb a molecule if $\xi \leqslant R$.

(ii) If the two sites are occupied by atoms belonging to the same molecule, then desorb the molecule if $\xi \leqslant R$.

(iii) Otherwise, the attempt is rejected.

$R = \min\{1, \exp(-\Delta H/k_B T)\}$ is the transition probability given by the Metropolis [45] rule, where $\Delta H = H_f - H_i$ is the difference between the Hamiltonians of the final and initial states and k_B is the Boltzmann constant. In addition, displacement (diffusional relaxation) of adparticles to nearest-neighbor positions, by either jumps along the dimer axis or reptation by rotation around the dimer end, must be allowed in order to reach equilibrium in a reasonable time. A MC step (MCS) is achieved when M pairs of sites have been tested to change its occupancy state. Typically, the equilibrium state can be well reproduced after discarding the first $r' = 5 \times 10^5$ MCS. Then, the next $r = 2 \times 10^5$ MCS's are used to compute averages.

Thermodynamic quantities such as mean coverage, θ, and mean adsorption energy per site, u, are obtained as simple averages:

$$\theta = 2\frac{\langle N\rangle}{M}, \tag{3}$$

$$u = \frac{1}{M}\langle H\rangle. \tag{4}$$

The differential heat of adsorption can be obtained from our simulation as [46–48]

$$q_d = -\frac{\partial u}{\partial \langle N\rangle}, \tag{5}$$

where the thermal average $\langle\cdots\rangle$ means the time average over the Monte Carlo simulation run.

III. THEORY

From a theoretical point of view, when intermolecular forces are introduced (in the present paper, NN denotes nonadditive interactions), an extra term in the partition function for interaction energy is required. With this extra term, only partition functions for the whole system can be written. Ising [49] gave an exact solution to the 1D monolayer in 1925. All other cases are expressed in terms of series solution [12,50], except for the special case of 2D monolayers at half-coverage, which was exactly solved by Onsager [51] in 1944. Close approximate solutions in dimensions higher than 1 can be obtained, and the two most important of these are the Bragg-Williams approximation (BWA) [12] and the quasichemical approximation (QCA) [12,52]. These leading models have played a central role in the study of adsorption systems in the presence of lateral interactions between the adatoms. Next, the BWA and the QCA will be applied to study monolayer adsorption of nonadditive interacting straight rigid rods.

A. Mean-field approximation for adsorbed *k*-mers

The Bragg-Williams approximation is the simplest mean-field treatment for interacting adsorbed particles, even in the case of nonadditive couplings and multisite occupancy. In this context, the canonical partition function $Q(M,N,T,P)$ for a system of $N k$-mers adsorbed on M sites at a temperature T, considering NN lateral interactions characterized by a nonadditivity parameter P, is given by

$$Q(N,M,T,P) = \sum_{\{E_k\}} \Omega(E_k) e^{-\beta[E_k(N,M,P)+NkU_0]}, \tag{6}$$

where $\Omega(E_k)$ is the total number of distinguishable configurations of N k-mers on M sites with lateral interaction energy E_k, NkU_0 accounts for the k-mer–lattice interaction energy, and $\beta = (k_B T)^{-1}$. If a mean-field approximation is introduced at this point,

$$\begin{aligned} Q(N,M,T,P) &= e^{-\beta[\overline{E}_k(N,M,P)+NkU_0]} \sum_{\{E_k\}} \Omega(E_k) \\ &= e^{-\beta[\overline{E}_k(N,M,P)+NkU_0]} \Omega(N,M,\gamma), \end{aligned} \tag{7}$$

where $\Omega(N,M,\gamma)$ is the number of configurations of $N k$-mers on a lattice with M sites and connectivity γ, and $\overline{E}_k(N,M,P)$ is the mean lateral interaction energy of the system assuming that the N k-mers are randomly distributed over M sites. $\Omega(N,M,\gamma)$ is calculated considering that the molecules are distributed completely at random on the lattice and assuming the arguments given by different authors [42,53,54] to relate the configurational factor $\Omega(N,M,\gamma)$ for any γ, with the same quantity in one dimension, $\gamma = 2$. Thus,

$$\Omega(M,N,\gamma) = K(\gamma,k)^N \Omega(M,N,2), \tag{8}$$

where $K(\gamma,k)$ is, in general, a function of the connectivity and the size of the molecules, and $\Omega(N,M,2)$ can be readily calculated [42] giving

$$\Omega(M,N,2) = \frac{[M-(k-1)N]!}{N![M-kN]!}. \tag{9}$$

In the particular case of straight rigid k-mers, it follows that $K(\gamma,k) = \gamma/2$.

On the other hand,

$$\overline{E}_k(N,M,P) = \frac{N}{2}\sum_{m=0}^{\lambda} m W_m P_m, \tag{10}$$

where $\lambda = (\gamma - 2)k + 2$ and P_m is the probability that a k-mer will be surrounded by m NN occupied sites [and $(\lambda - m)$ NN empty sites], which can be written in terms of the mean coverage $\theta = kN/M$,

$$P_m = \binom{\lambda}{m}\left(\frac{kN}{M}\right)^m \left(1 - \frac{kN}{M}\right)^{\lambda - m}. \tag{11}$$

Then,

$$\overline{E}_k(N,M,P) = \frac{N}{2}\sum_{m=0}^{\lambda} m W_m \binom{\lambda}{m}\left(\frac{kN}{M}\right)^m \left(1 - \frac{kN}{M}\right)^{\lambda - m}. \tag{12}$$

From Eq. (12) and using the expression (2), one obtains

$$\overline{E}_k(N,M,P)=\frac{\lambda WN}{2}\left[P\left(\frac{kN}{M}\right)+(1-P)\left(\frac{kN}{M}\right)^2\right]. \tag{13}$$

Hence, the canonical partition function $Q(N,M,T,P)$ can be written as

$$Q(N,M,T,P)=\left(\frac{2}{\gamma}\right)^N\frac{(M-(k-1)N)!}{N!(M-kN)!}\times e^{\frac{-\beta\lambda WN}{2}[P(\frac{kN}{M})+(1-P)(\frac{kN}{M})^2]}, \tag{14}$$

where U_0 has been set equal to zero without any loss of generality.

The Helmholtz free energy $F(M,N,T,P)$ is given by

$$\begin{aligned}\beta F&(N,M,T,P)\\ &=-\ln[Q(N,M,T,P)]\\ &=-\ln[(M-(k-1)N)!]+\ln N!+\ln[(M-kN)!]\\ &-N\ln\left(\frac{2}{\gamma}\right)+\frac{\beta W\lambda N}{2}\left[P\left(\frac{kN}{M}\right)+(1-P)\left(\frac{kN}{M}\right)^2\right].\end{aligned} \tag{15}$$

The Helmholtz free energy per site can be obtained as a function of coverage θ and temperature T,

$$\begin{aligned}\beta f(\theta,T,P)&=\frac{\beta F(N,M,T,P)}{M}\\ &=\left[\left(\frac{k-1}{k}\right)\theta-1\right]\ln\left[1-\left(\frac{k-1}{k}\right)\theta\right]\\ &\quad+\frac{\theta}{k}\ln\left[\frac{\theta}{k}\right]+(1-\theta)\ln(1-\theta)\\ &\quad-\frac{\theta}{k}\ln\left(\frac{2}{\gamma}\right)+\frac{\beta W\lambda\theta}{2k}[P\theta+(1-P)\theta^2].\end{aligned} \tag{16}$$

Then, all the equilibrium properties of the adlayer can be deduced from Eq. (16) along with the differential form of F in the canonical ensemble,

$$dF=-SdT-\pi dM+\mu dN, \tag{17}$$

where S, π, and μ represent the entropy, the spreading pressure, and the chemical potential, respectively.

Thus, the coverage dependence of the chemical potential, $\mu[=(\partial F/\partial N)_{M,T}]$, arises straightforwardly from Eqs. (16) and (17),

$$\beta\mu=\ln\left\{\frac{2\theta\left[1-\theta\left(\frac{k-1}{k}\right)\right]^{k-1}}{\gamma k(1-\theta)^k}\right\}+\frac{\beta W\lambda}{2}[2P\theta+3(1-P)\theta^2]. \tag{18}$$

The configurational energy per site, u, can be calculated as

$$u=\frac{\overline{E}_k(N,M,P)}{M}=\frac{\lambda W\theta}{2k}[P\theta+(1-P)\theta^2]. \tag{19}$$

Finally, the differential heat of adsorption q_d is defined as

$$\frac{q_d}{k_BT^2}=\left(\frac{\partial\beta\mu}{\partial T}\right)_\theta=-\frac{W\lambda}{2k_BT}[2P\theta+3(1-P)\theta^2]. \tag{20}$$

In the case of $k=1$ [and $K(\gamma,k=1)=1$], the present results reproduce those of Milchev and Paunov [35]. Namely,

$$u=\frac{\gamma W\theta}{2}[P\theta+(1-P)\theta^2] \tag{21}$$

and

$$\beta\mu=-\frac{\beta\gamma W}{2}[3(1-P)\theta^2+2P\theta]+\ln\left(\frac{\theta}{1-\theta}\right). \tag{22}$$

On the other hand, if $P=1$, Eqs. (16), (18), and (20) reduce to the corresponding thermodynamic functions obtained by Ramirez-Pastor *et al.* [55] for additive interacting chains:

$$\begin{aligned}\beta f(\theta,T,P)&=\left[\left(\frac{k-1}{k}\right)\theta-1\right]\ln\left[1-\left(\frac{k-1}{k}\right)\theta\right]\\ &\quad+\frac{\theta}{k}\ln\left(\frac{\theta}{k}\right)+(1-\theta)\ln(1-\theta)\\ &\quad-\frac{\theta}{k}\ln\left(\frac{2}{\gamma}\right)+\frac{\beta W\lambda\theta^2}{2k},\end{aligned} \tag{23}$$

$$\beta\mu=\ln\left\{\frac{2\theta\left[1-\theta\left(\frac{k-1}{k}\right)^{k-1}\right]}{\gamma k(1-\theta)^k}\right\}+\beta W\lambda\theta, \tag{24}$$

and

$$\frac{q_d}{k_BT^2}=-\frac{W\lambda\theta}{k_BT}. \tag{25}$$

B. Quasichemical approximation for straight rigid rods

In this section, we describe the quasichemical approach. As was demonstrated in previous work [43], the QCA leads to an approximation significantly better than the BWA and, at the same time, mathematically manageable.

As is well known, the essence of the QCA is that pairs of nearest-neighbor sites are treated as independent of each other. Then, in order to apply the configuration-counting procedure of the QCA, it is convenient to write Eq. (26) in terms of the number of pairs of nearest-neighbor sites. Thus,

$$Q(N,M,T,P)=\sum_{N_{11}}\Omega(N,M,N_{11})e^{-\beta[E_k(N,M,N_{11},P)+NkU_0]}, \tag{26}$$

where q is the partition function for a single adsorbed molecule, N_{11} is the number of pairs of NN units belonging to different k-mers, $E_k(N,M,N_{11},P)$ is the lateral interaction energy corresponding to N k-mers on M sites with N_{11} pair of occupied sites, and $\Omega(N,M,N_{11})$ is the number of ways to array N k-mers on M sites with N_{11} pair of occupied sites.

As is usual in the case of single-site occupation, it is convenient to write the canonical partition function as a function of N_{01}, where N_{01} is the number of pairs formed by an empty site adjacent to an occupied site. For this purpose, the relations between N_{11}, N_{01}, and N_{00} (N_{00} being the number of pairs of empty NN sites) are calculated:

$$2N_{11}+N_{01}+2N(k-1)=\gamma kN, \tag{27}$$

$$2N_{00}+N_{01}=\gamma(M-kN), \tag{28}$$

where “number of 01 pairs” = “number of 10 pairs” = $N_{01}/2$. In the case of $k = 1$, the well-known relations for single-site occupation are recovered [12].

Now, the canonical partition function can be written in terms of N_{01},

$$Q(N,M,T,P) = \sum_{N_{10}} \Omega(N,M,N_{10}) e^{-\beta[E_k(N,M,N_{10},P)+NkU_0]}. \tag{29}$$

In addition, the configurational energy can be written as

$$E_k(N,M,N_{10},P) = \frac{N}{2}\sum_{m=0}^{\lambda} m W_m P_m, \tag{30}$$

where U_0 has been set equal to zero without any loss of generality.

To obtain P_m [probability that a k-mer will be surrounded by m NN occupied sites and $(\lambda - m)$ NN empty sites], we use a generalization of the standard QCA procedure for monomers [38]. Since there are N k-mers on the surface, a total of $\lambda N/2$ (the factor $1/2$ avoids double counting the pairs) pairs of sites may either be of the type N_{11} or of the type N_{10}. Then, the probability of a single pair to be of the type N_{11} or N_{10} (or N_{01}) is $N_{11}/(\lambda N/2)$ or $(N_{10}/2)/(\lambda N/2)$, respectively . According to the QCA, these probabilities are considered to be independent, and, consequently, P_m can be written as

$$P_m = \binom{\lambda}{m}\left[\frac{N_{11}}{\frac{\lambda}{2}N}\right]^m \left[\frac{N_{10}}{\lambda N}\right]^{\lambda-m}. \tag{31}$$

Introducing Eq. (31) in Eq. (30), using the relation $N_{11} = \lambda N/2 - N_{10}/2$ [see Eq. (27)], and denoting the concentration of N_{10} pairs by $X = N_{10}/(\lambda N)$, we have

$$E_k(N,M,N_{10},P) = \frac{N}{2}\sum_{m=0}^{\lambda} m \binom{\lambda}{m} W_m (1-X)^m (X)^{\lambda-m}. \tag{32}$$

By simple algebra, Eq. (32) may be put down in a more convenient form as a λth degree polynomial in X,

$$E_k(N,M,N_{10},P) = \frac{N}{2}\sum_{h=0}^{\lambda} \alpha_h X^h \tag{33}$$

with

$$\alpha_h = \sum_{n=0}^{h} (\lambda - h + n)\binom{\lambda}{\lambda - h + n}\binom{\lambda - h + n}{\lambda - h} \times (-1)^{\lambda-n} W_{\lambda-h+n}. \tag{34}$$

From Eqs. (33) and (34) and using expression (2), we obtain

$$\begin{aligned} E_k(N,M,N_{10},P) &= \frac{N}{2}(\alpha_0 + \alpha_1 X + \alpha_2 X^2) \\ &= \frac{N}{2}[\lambda W_\lambda (-1)^\lambda + \{\lambda(\lambda-1) W_{\lambda-1}(-1)^\lambda + \lambda^2 W_\lambda (-1)^{\lambda-1}\} X] \\ &\quad + \frac{N}{2}\left[\left\{\frac{\lambda(\lambda-1)(\lambda-2)}{2} W_{\lambda-2}(-1)^\lambda \right.\right. \\ &\quad \left.\left. + \frac{\lambda(\lambda-1)^2}{2} W_{\lambda-1}(-1)^{\lambda-1}\right\} X^2\right] \\ &\quad + \frac{N}{2}\left[\left\{\frac{\lambda^2(\lambda-1)}{2} W_\lambda (-1)^{\lambda-2}\right\} X^2\right]. \end{aligned} \tag{35}$$

We shall now calculate the configurational factor. By using the standard formalism of the QCA, the number of ways of assigning a total of $[\gamma M/2 - N(k-1)]$ independent pairs[3] to the four categories 11, 10, 01, and 00, with any number 0 through $[\gamma M/2 - N(k-1)]$ per category consistent with the total, is

$$\begin{aligned} \widetilde{\Omega}(N,M,N_{10}) &= \frac{\left[\frac{\gamma M}{2} - N(k-1)\right]!}{N_{11}!(N_{10}!)^2 N_{00}!} \\ &= \frac{\left[\frac{\gamma M}{2} - N(k-1)\right]!}{(N_{10}!)^2 \left(\frac{\gamma(M-kN)}{2} - \frac{N_{01}}{2}\right)! \left(\frac{\lambda N}{2} - \frac{N_{01}}{2}\right)!}. \end{aligned} \tag{36}$$

This cannot be set equal to $\Omega(N,M,N_{01})$ in Eq. (29), because treating the pairs as independent entities leads to some unphysical configurations (see Ref. [12], p. 253). Thus, $\widetilde{\Omega}$ overcounts the number of configurations. To take care of this, we must normalize $\widetilde{\Omega}$ as

$$\Omega(N,M,N_{10}) = C(N,M)\widetilde{\Omega}(N,M,N_{10}) \tag{37}$$

and

$$\Omega(N,M) = \sum_{N_{10}} \Omega(N,M,N_{10}) = C(N,M)\sum_{N_{10}} \widetilde{\Omega}(N,M,N_{10}), \tag{38}$$

where $\Omega(N,M)$ is the number of ways to arrange Nk-mers on M sites. In general, $\Omega(N,M)$ depends on the spatial configuration of the k-mer and the surface geometry. Even in the simplest case of linear k-mers, there does not exist an exact form of $\Omega(N,M)$ in two (or more) dimensions.[4] However, different approximations have been developed for $\Omega(N,M)$ [56], which allow us to obtain $C(N,M)$.

By operating as in Ref. [43], we obtain

$$C(N,M) = \Omega(N,M)\left\{\frac{\left[M - 2(k-1)\frac{N}{\gamma} - \frac{\lambda N}{\gamma}\right]!\left(\frac{\lambda N}{\gamma}\right)!}{\left[M - 2(k-1)\frac{N}{\gamma}\right]!}\right\}. \tag{39}$$

Now, $\ln Q(N,M,T,P)$ can be written as

$$\begin{aligned} \ln Q(N,M,T,P) \\ = \ln\left\{\sum_{N_{10}} C(N,M)\widetilde{\Omega}(N,M,N_{10}) e^{-\beta[E_k(N,M,N_{10},P)]}\right\}. \end{aligned} \tag{40}$$

---

[3] The term $N(k-1)$is subtracted since the total number of NN pairs, $\gamma M/2$, includes the $N(k-1)$ bonds belonging to the N adsorbed k-mers.

[4] In the case $c = 2$ (one-dimensional lattice), it is possible to write $\Omega(N,M) = [M - (k-1)N]!/[N!(M-kN)!]$, which is an exact result.

In order to solve Eq. (40), we replace $\sum_{N_{01}} C(N,M)\tilde{\Omega}(N,M,N_{01})\exp[-\beta E_k(N,M,N_{10},P)]$ by the maximum term in the sum, $C(N,M)\tilde{\Omega}(N,M,N_{01}^{**})\exp[-\beta E_k(N,M,N_{01}^{**},P)]$. Thus,

$$\begin{aligned}\ln Q(N,M,T,P) = &+\left[1-\frac{2(k-1)N}{\gamma M}-\frac{\lambda N}{\gamma M}+\frac{N}{M}\right]\ln\left[1-\frac{2(k-1)N}{\gamma M}-\frac{\lambda N}{\gamma M}+\frac{N}{M}\right]\\ &-\frac{N}{M}\ln\left(\frac{N}{M}\right)+(\gamma-1)\left[1-\frac{2(k-1)N}{\gamma M}-\frac{\lambda N}{\gamma M}\right]\ln\left[1-\frac{2(k-1)N}{\gamma M}-\frac{\lambda N}{\gamma M}\right]\\ &+\frac{\lambda N}{M}\ln\left(\frac{\lambda N}{M}\right)-\gamma\left[1-\frac{2(k-1)N}{\gamma M}\right]\ln\left[1-\frac{2(k-1)N}{\gamma M}\right]\\ &+\frac{\gamma}{2}\left[1-\frac{2(k-1)N}{\gamma M}\right]\ln\left\{\frac{\gamma}{2}\left[1-\frac{2(k-1)N}{\gamma M}\right]\right\}-N_{01}^{**}\ln\left(\frac{N_{01}^{**}}{2}\right)\\ &-\left\{\frac{\gamma}{2}\left[1-\frac{2(k-1)N}{\gamma M}\right]-\frac{\lambda N}{2M}-\frac{N_{01}^{**}}{2}\right\}\ln\left\{\frac{\gamma}{2}\left[1-\frac{2(k-1)N}{\gamma M}\right]-\frac{\lambda N}{2M}-\frac{N_{01}^{**}}{2}\right\}\\ &-\left(\frac{\lambda N}{2M}-\frac{N_{01}^{**}}{2}\right)\ln\left(\frac{\lambda N}{2M}-\frac{N_{01}^{**}}{2}\right)-\frac{\beta kNW}{2M}\left[(P-2)M\frac{N_{01}^{**}}{N}+\frac{(1-P)}{\lambda}\left(M\frac{N_{01}^{**}}{N}\right)^2+\lambda\right],\end{aligned}\tag{41}$$

where N_{01}^{**} is obtained from the maximization condition

$$\left[\gamma-\frac{2(k-1)N}{M}-\frac{\lambda N}{M}-N_{01}^{**}\right]\left(\frac{\lambda N}{M}-N_{01}^{**}\right)=N_{01}^{**}\exp\left[\frac{\beta}{\lambda}\left(A+\frac{N_{01}^{**}2BM}{\lambda N}\right)\right],\tag{42}$$

with

$$A=\lambda(\lambda-1)W_{\lambda-1}(-1)^{\lambda}+\lambda^2W_{\lambda}(-1)^{\lambda-1}\tag{43}$$

and

$$B=\frac{\lambda(\lambda-1)(\lambda-2)}{2}W_{\lambda-2}(-1)^{\lambda}+\frac{\lambda(\lambda-1)^2}{2}W_{\lambda-1}(-1)^{\lambda-1}+\frac{\lambda^2(\lambda-1)}{2}W_{k}(-1)^{\lambda-2}.\tag{44}$$

Following the scheme in Eqs. (15)–(20), the chemical potential μ, the configurational energy per site u, and the differential heat of adsorption q_d can be calculated in terms of the intensive variables θ and $\delta = N_{01}^{**}/2M$. Then,

$$\beta\mu=-\beta\frac{W}{2}\left[\frac{(1-P)4\delta^2k^2}{\lambda\theta^2}-\lambda\right]+\ln\left\{\frac{\theta}{k}\left(\frac{\gamma}{2}\right)^{2k-3}\frac{(1-\theta)^{k(\gamma-1)}\,[k-(k-1)\theta]^{k-1}\left(\frac{\lambda\theta}{2k}-2\delta\right)^{\frac{\lambda}{2}}}{\left[\frac{\gamma k}{2}-(k-1)\theta\right]^{k-1}\left[\frac{\gamma}{2}(1-\theta)-2\delta\right]^{\frac{\gamma k}{2}}\left(\frac{\lambda\theta}{\gamma k}\right)^{\lambda}}\right\},\tag{45}$$

$$u=\frac{\theta W\lambda}{2k}\left[1+(P-2)\frac{2\delta}{\lambda\theta}+(1-P)\left(\frac{2\delta}{\lambda\theta}\right)^2\right],\tag{46}$$

and

$$\frac{q_d}{k_BT^2}=\frac{W\lambda}{2k_BT^2}\left[\frac{4(1-P)\delta^2k^4}{\lambda^3\theta^3}-\lambda\right]-\left\{\frac{4W(1-P)\delta^4k^4}{k_BT\lambda^3\theta^3}-\frac{1}{2}\left[\frac{\lambda}{\frac{\lambda\theta}{k}-\frac{2k\delta}{\lambda\theta}}-\frac{\lambda k}{\lambda(1-\theta)-\frac{2k\delta}{\lambda\theta}}\right]\right\}\frac{2k}{\lambda\theta}\left(\frac{\partial\delta}{\partial T}\right)_{\theta},\tag{47}$$

where $(\partial\delta/\partial T)_\theta$ is obtained from Eqs. (42):

$$\left(\frac{\partial\delta}{\partial T}\right)_{\theta}=\frac{-\left(\frac{2k}{\lambda\theta}\right)\delta^2\beta^2W\left[P-2+\frac{4k^2\delta(1-P)}{\lambda^2\theta^2}\right]\exp\left\{\beta W\left[P-2+\frac{4k^2\delta^2(1-P)}{\lambda^2\theta^2}\right]\right\}}{\frac{4k\delta}{\lambda\theta}-\lambda+\frac{2\theta(k-1)}{k}-\left[\frac{2k\delta}{\lambda\theta}+\beta\left(\frac{2k}{\lambda\theta}\right)^3W\delta^2(1-P)\right]\exp\left\{\beta W\left[P-2+\frac{4k^2\delta(1-P)}{\lambda^2\theta^2}\right]\right\}}.\tag{48}$$

Two well-known limit cases can be obtained from Eq. (45): (i) for $k = 1$, Eq. (45) reproduces previous results for nonadditive monomers [38]; and (ii) for $P = 1$, Eq. (45) reduces to the expression of the adsorption isotherm of additive interacting k-mers in the QCA framework [43].

IV. RESULTS

In the present section, the main characteristics of the thermodynamic functions given in Eqs. (18)–(20) and Eqs. (45)–(48) will be analyzed in comparison with simulation results for a lattice gas of interacting dimers[5] on one- and two-dimensional lattices.

The computational simulations have been developed for one-dimensional chains of 10^4 sites and square $L \times L$ lattices with $L = 144$ and periodic boundary conditions. With this

---

[5] The dimer is the simplest case of a straight rigid rod and contains all the properties of the multisite-occupancy adsorption.

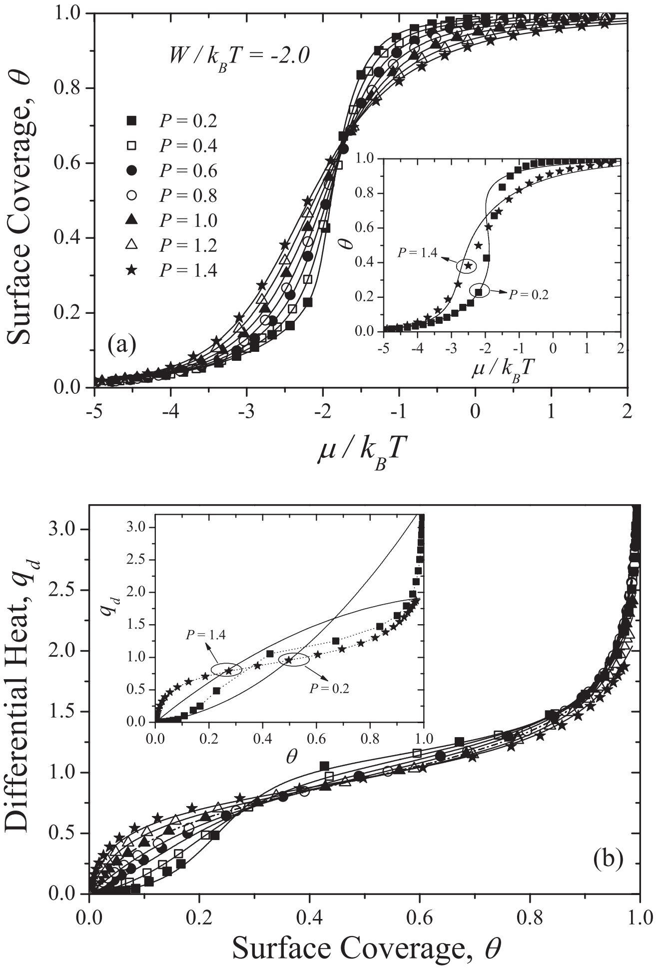

FIG. 2. (a) Adsorption isotherms and (b) differential heat of adsorption (for homonuclear dimers adsorbed on a one-dimensional lattice) with attractive NN interactions ($W/k_BT = -2$) and different values of the nonadditivity parameter, P, as indicated. Symbols represent Monte Carlo simulations and solid lines correspond to theoretical results from QCA. Inset: comparison between MC simulation (symbols) and BWA (dotted line) for the two limit cases $P = 0.2$ and 1.4.

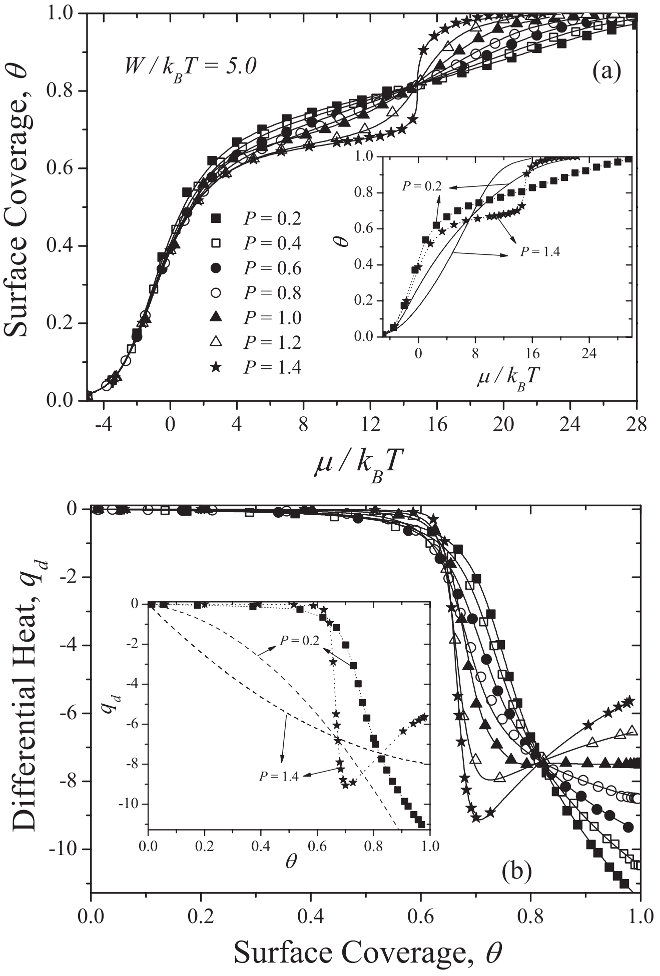

FIG. 3. As Fig. 2 for repulsive NN interactions ($W/k_BT = 5$).

lattice size, we verified that finite-size effects are negligible. Note, however, that the linear dimension L has to be properly chosen such that the adlayer structure is not perturbed.

For comparison purposes and even though the problem of k-mers adsorbed on a line could be solved by using the transfer-matrix technique, it is instructive to begin by discussing the behavior of the one-dimensional case (Figs. 2 and 3), where two k-mers interact through their ends. From an experimental point of view, numerous studies of gas adsorption on nanotube bundles suggest that the admolecules form one-dimensional systems or lines when adsorbed within interstitial channels [57,58] or along the groove sites [59–61]. There have also been reports of the one-dimensional character of adsorption in grooves of surface crystal planes of TiO_2 [62] and adsorption of alkane binary mixture in zeolites [63].

Figure 2 shows (a) the adsorption isotherms and (b) the differential heat of adsorption for homonuclear dimers adsorbed on a one-dimensional lattice with attractive NN interactions ($W/k_BT = -2$) and different values of the nonadditivity parameter, P.

In the case $P = 1$, the corresponding curve reduces to the rigorous adsorption isotherm of interacting dimers adsorbed flat on a one-dimensional lattice (additive case). The weaker the nonadditivity parameter, the steeper the adsorption isotherm for attractive dimers becomes. This behavior can be understood considering $W_m(P)$ as shown in Eq. (2). For $P < 1$ (and $W < 0$), $W_2 < W_1$, and consequently (i) each adparticle prefers to have its two neighboring sites occupied, and (ii) the slope of the adsorption isotherm increases. On the other hand, $W_2 > W_1$ as $P > 1$ (and $W < 0$), and a sequential adsorption, increasing the number of nearest neighbors, is observed. The differential heat of adsorption as a function of coverage [part (b) of Fig. 2] follows the behavior of the adsorption isotherms.

With respect to the theoretical approximations, MC simulations in the grand-canonical ensemble (symbols) fully agree with the predictions from the QCA (solid lines). In the inset, the limit cases in Fig. 2 ($P = 0.2$ and 1.4) are compared with results from the BWA. As can be observed, the disagreement between MC and the BWA turns out to be significantly large. For $P = 0.2$, a characteristic van der Waals loop is observed in the theoretical adsorption isotherm, and the BWA incorrectly predicts a phase transition in one dimension.

The behavior of repulsive interacting dimers (Fig. 3) is completely different. In order to understand the basic phenomenology, we consider in the first place $P = 1$, where the model reduces to the additive interaction scheme. In this case, dimers avoiding configurations with nearest-neighbor repulsive heads order in a structure of alternating dimers separated by an empty site at $\theta = 2/3$. The width of the step is directly proportional to the energy per dimer necessary to alter such an ordered structure.

Two different behaviors are observed according to the value of P: (a) $P < 1.0$ and (b) $P > 1.0$. For $P < 1$ (and $W > 0$), $W_2 > W_1$ and the sequential filling of the lattice smooths the plateau at $\theta = 2/3$.

For $P > 1$ (and $W > 0$), $W_2 < W_1$. Then, each incoming adparticle adsorbs on the surface avoiding the formation of isolated pairs of dimers. This reinforces the plateau at $\theta = 2/3$ in the adsorption isotherm (step in the differential heat of adsorption) and produces a jump in the coverage when the fraction of NN dimers changes abruptly from 0 (isolated dimers and $\theta = 2/3$) to 1 (each dimer possesses two neighbor dimers and $\theta = 1$). Consequently, the isotherms show the characteristic appearance of attractive interactions. This striking behavior is indicative that, even in the presence of only repulsive interactions, marked jumps in the adsorption isotherms can be observed for nonadditive interactions.

As in Fig. 2, results from the QCA fully agree with the MC data. With respect to the BWA, the curves in the insets of Figs. 3(a) and 3(b) show that appreciable differences can be seen between simulation and mean-field theoretical results.

Figures 2 and 3 allow us to validate the theory and the MC scheme. Hereafter, we present the analysis of the adsorption thermodynamics of nonadditive interacting dimers on two dimensions.

For the analysis of two-dimensional systems, the adsorption on square lattices is studied. For such a geometry, each dimer has six nearest-neighbor sites, and consequently m Eq. (2) varies between 1 and 6. We analyze the system for two cases: attractive and repulsive interactions. For the first case, Fig. 4 shows the adsorption isotherms at several values of P and $W/k_BT = -1$. Symbols represent MC data and solid lines correspond to theoretical results from the QCA. As discussed in Fig. 2, the slope of the MC curves increases as the nonadditivity parameter P decreases. In the case of the figure, for values of P below $P \approx 0.6$, the system undergoes a first-order phase transition (with a clustering of the adparticles), which is observed in the clear discontinuity in the adsorption isotherms. In this situation, which has been reported experimentally in numerous systems, the only phase that one expects is a lattice-gas phase at low coverage, separated by a two-phase coexistence region from a "lattice-fluid" phase at higher coverage.

One important conclusion can be drawn from the study in Fig. 4: the critical temperature characterizing the gas-fluid phase transition occurring in the system depends on the nonadditivity parameter P. In other words, an effect of nonadditivity is to modify the critical point of the system.

Both theoretical approximations present the characteristic van der Waals loop at a critical regime, with the QCA being the most accurate for all cases. This situation is clearly reflected in the inset of Fig. 4, where a comparison between MC (symbols), QCA (solid lines), and BWA (dashed lines) results is shown for the limit cases corresponding to $P = 0.2$ and 1.6.

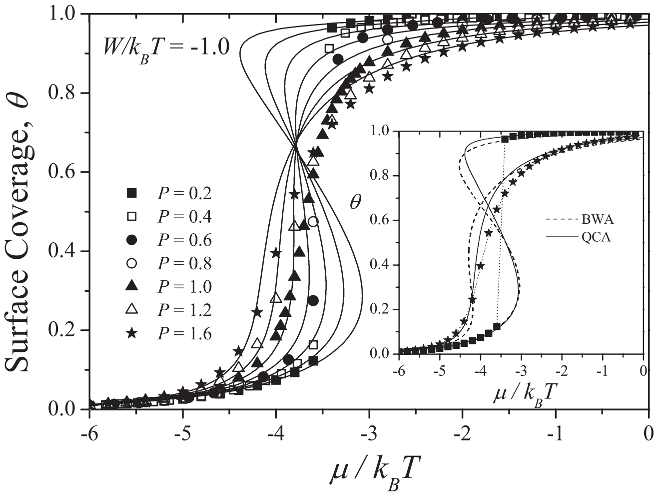

FIG. 4. Adsorption isotherms for homonuclear dimers adsorbed on a square lattice with attractive NN interactions ($W/k_BT = -1$) and different values of the nonadditivity parameter, P, as indicated. Symbols represent Monte Carlo simulations and lines correspond to theoretical results from QCA. Inset: Comparison between MC simulation (symbols), QCA (solid lines), and BWA (dashed lines) curves for the limit cases corresponding to $P = 0.2$ and 1.6.

In Fig. 5, we present the results of the adsorption isotherms for repulsive interactions. The notation is as in Fig. 4. At the additive situation ($P = 1$), the MC curve shows the formation of two well-defined and pronounced steps. The first step appearing at $\theta = 1/2$ corresponds to a (4×2) ordered structure, characterized by alternating files of dimers separated by two adjacent empty sites. The (4×2) phase resembles the well-known $c(2 \times 2)$ structure for adsorbed monomers with repulsive nearest-neighbor interactions [43]. The second step at $\theta = 2/3$ corresponds to the so-called zigzag structure. In

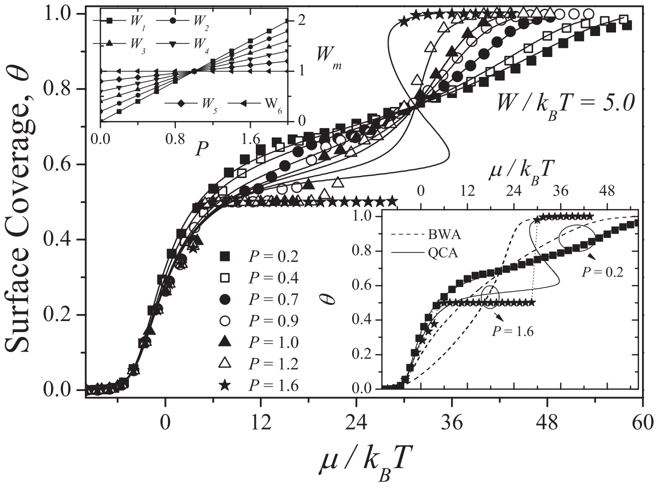

FIG. 5. As Fig. 4 for repulsive NN interactions ($W/k_BT = 5$). Upper-left inset: Adsorbate-adsorbate interaction W_m as a function of the nonadditivity parameter P. Lower-right inset: Comparison between MC simulation (symbols), QCA (solid lines), and BWA (dashed lines) curves for the limit cases corresponding to $P = 0.2$ and 1.6.

this case, the dimers are adsorbed forming domains of zigzag one-dimer-width strips at ±45 from the lattice symmetry axes, separated from each other by single-site empty channels. The periodicity of the zigzag varies from 1 to L [43].

The (4×2) and zigzag structures are also present for nonadditive interactions. For $P < 1$ ($P > 1$), the structure at coverage 1/2 (2/3) is weakened (reinforced). In other words, the first (second) plateau at $\theta = 1/2$ ($\theta = 2/3$) is less (more) wide upon decreasing (increasing) P. In the limit conditions, the plateau at coverage 1/2 (2/3) disappears for $P = 0.2$ ($P = 1.6$).

An unusual feature is observed for values of the nonadditivity parameter larger than 1. Under these conditions, the adsorption isotherms exhibit discontinuities, i.e., jumps of the surface coverage. These discontinuities correspond to first-order phase transitions between surface phases at low and high densities. This phenomenon, which has also been reported in the adsorption of nonadditive monomers [39–41], can be explained by considering $W_m(P)$ as it is shown in the upper-left inset of the figure. For $P > 1$ (and $W > 0$), $W_6 < W_i$ ($i = 1,2,3,4,5$) and the system prefers to condensate in such a way that each adsorbed dimer possesses six nearest-neighbor occupied sites in contrast with a sequential adsorption increasing the number of nearest-neighbor occupied sites upon raising the chemical potential, as occurs for $P < 1$.

There exists a wide range of P's ($0.2 \leqslant P \leqslant 1$), where the QCA (solid lines) provides an excellent fit to the simulation data. For $P > 1.0$, the QCA presents a typical van der Waals loop, in correspondence with the condensation observed at high densities.

To complete the description of Fig. 4, the lower-right inset shows a comparison between MC simulation (symbols), QCA (solid lines), and BWA (dashed lines) curves for the limit cases corresponding to $P = 0.2$ and 1.6. The differences between the QCA and the BWA are very appreciable, and the BWA does not predict the existence of structures in the adsorbate, nor the phenomenon of condensation. These findings (i) show that the QCA represents a qualitative advance in the description of the adsorption of nonadditive k-mers with respect to the existing theories based on the mean-field approximation; and (ii) suggest the potentiality of the model proposed in supporting the interpretation of experimental data in the presence of multisite occupancy and nonadditive interactions.

The differences between numerical and theoretical results can be rationalized with the help of the absolute error, $\varepsilon^a(\theta)$, which is defined as

$$\varepsilon^a(\theta) = |\mu_{\rm MC} - \mu_{\rm theory}|_\theta, \tag{49}$$

where $\mu_{\rm MC}$ ($\mu_{\rm theory}$) represents the chemical potential obtained by using the MC simulation (analytical approach). Each pair of values ($\mu_{\rm MC}$, $\mu_{\rm theory}$) is obtained at fixed θ.

For attractive interactions and different values of P, it can be concluded that, in all cases, the QCA leads to appreciably better results than the BWA. In the case of repulsive interactions, the differences between the QCA and the BWA are largely enhanced. These findings can be visualized more easily by using the integral error ε^i, which takes into account the differences between theoretical and simulation data in all ranges of coverage. It can be defined by

$$\varepsilon^i(\theta) = \int_0^1 \varepsilon^a(\theta) d\theta. \tag{50}$$

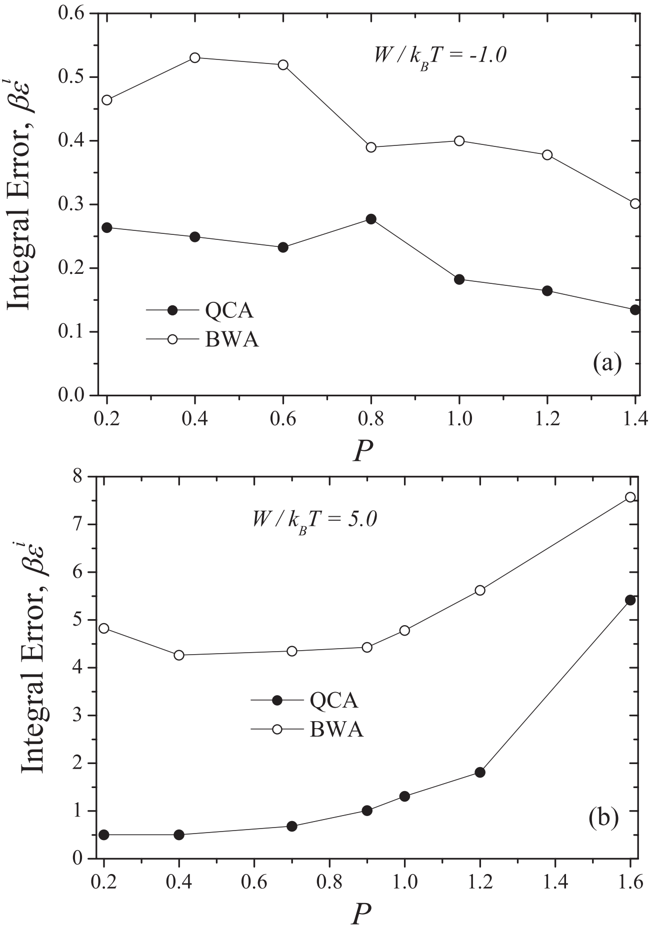

FIG. 6. Integral error in k_BT units, $\beta\varepsilon^i$, vs the nonadditivity parameter for attractive [part (a)] and repulsive [part (b)] NN interactions. Full and open symbols correspond to comparisons with QCA and BWA, respectively.

Thus, the integral error is shown in Fig. 6 for all studied cases: attractive interactions, part (a); repulsive interactions, part (b). In all cases, the QCA gives a much better description of the MC adsorption isotherms than the BWA. In the particular case of repulsive interactions, the disagreement between MC and the BWA turns out to be significantly large, while the QCA appears to be the simplest approximation capable of taking into account the main features of the existence of nonadditive lateral interactions.

Beyond the quantitative discrepancies between the QCA and the BWA, there exist qualitative differences between both approximations. Thus, while the BWA does not predict the existence of ordered phases in the adsorbate, QCA isotherms present a pronounced plateau as the temperature lowers. Therefore, the QCA not only represents a qualitative advance in the description of the adsorption nonadditive k-mers with respect to the BWA, but it also gives a framework and compact equations to consistently interpret thermodynamic adsorption experiments in the presence of multisite occupancy and nonadditive interactions.

V. CONCLUSIONS

A generalization of the Bragg-Williams and quasichemical approximations for nonadditive interacting straight rigid rods on homogeneous surfaces has been presented. The main thermodynamic functions of adsorption (adsorption isotherm, configurational energy, isosteric heat of adsorption, and configurational entropy of the adlayer) have been calculated and compared with MC simulation data for a lattice gas of nonadditive interacting dimers on one-dimensional and square lattices.

The new formalism leads to exact results in one dimension, provides a close approximation for two-dimensional systems taking into account multisite occupancy and nonadditive lateral interactions, and shows the asymmetry observed in many experimental phase diagrams. From the comparison with MC simulations, the differences between QCA and BWA are very appreciable, QCA being the most accurate for all cases.

Beyond the quantitative discrepancies between QCA and BWA, there exist qualitative differences between both approximations. Thus, BWA does not predict the existence of structures in the adsorbate or the phenomenon of condensation (sharp discontinuities in the adsorption isotherms) in the presence of repulsive interactions. This unusual finding, which is a clear signal of the existence of nonadditive lateral interactions, reinforces the validity of the proposed QCA to describe nonadditive k-mers adsorption thermodynamics.

In summary, the proposed model is simple and seems to be a promising way toward a more accurate description of the adsorption thermodynamics of nonadditive k-mers. In this sense, future efforts will be directed to (i) study the critical behavior of the system for attractive and repulsive interactions; (ii) extend the calculations to kinetic properties as a diffusion coefficient, thermal desorption, etc.; and (iii) consider different forms for $g(N,M)$ in Eq. (38), analyzing its influence on the thermodynamic functions.

ACKNOWLEDGMENTS

This work was supported in part by CONICET (Argentina) under Project No. PIP 112-200801-01332, Universidad Nacional de San Luis (Argentina) under Project No. 322000, and the National Agency of Scientific and Technological Promotion (Argentina) under Project No. PICT-2010-1466. The numerical work was done using the parallel cluster BACO of Universidad Nacional de San Luis, Argentina. This facility consists of 60 PC's each with a 3.0 GHz Pentium-4 processor and 120 PC's each with a 2.4 GHz Intel Core 2 Quad processor.

---

[1] B. Crittenden and W. J. Thomas, *Adsorption Technology and Design* (Butterworth-Heinemann, Oxford, 1998).

[2] J. U. Keller and R. Staudt, *Gas Adsorption Equilibria: Experimental Methods and Adsorptive Isotherms* (Springer Science, New York, 2005).

[3] W. A. Steele, *The Interaction of Gases with Solid Surfaces* (Pergamon, New York, 1974).

[4] J. G. Dash, *Films on Solid Surfaces* (Academic, New York, 1975).

[5] J. G. Dash and J. Ruvalds, *Phase Transitions in Adsorbed Films* (Plenum, New York, 1980).

[6] S. K. Shina, *Ordering in Two Dimensions* (Elsevier, New York, 1980).

[7] K. Binder and D. P. Landau, Surf. Sci. **61**, 576 (1976).

[8] A. Patrykiejew, S. Sokolowski, and K. Binder, Surf. Sci. Rep. **37**, 207 (2000).

[9] V. P. Zhdanov, *Elementary Physicochemical Processes on Solid Surfaces* (Plenum, New York, 1991).

[10] W. Rudziński, W. A. Steele, and G. Zgrablich, *Equilibria and Dynamics of Gas Adsorption on Heterogeneous Solid Surfaces* (Elsevier, Amsterdam, 1996).

[11] J. L. Riccardo, F. Romá, and A. J. Ramirez-Pastor, Int. J. Mod. Phys. B **20**, 4709 (2006).

[12] T. L. Hill, *An Introduction to Statistical Thermodynamics* (Addison-Wesley, Reading, MA, 1962).

[13] A. Boutin, R. J.-M. Pellenq, and D. Nicholson, Chem. Phys. Lett. **219**, 484 (1994).

[14] V. Lachet, A. Boutin, R. J.-M. Pellenq, D. Nicholson, and A. H. Fuchs, J. Phys. Chem. **100**, 9006 (1996).

[15] R. Radhakrishnan and K. E. Gubbins, Phys. Rev. Lett. **79**, 2847 (1997).

[16] T. Maris, T. J. H. Vlugt, and B. Smit, J. Phys. Chem. B **102**, 7183 (1998).

[17] C. Martin, N. Tosi-Pellenq, J. Patarin, and J. P. Coulomb, Langmuir **14**, 1774 (1998).

[18] P. Zeppenfeld, J. George, V. Diercks, R. Halmer, R. David, G. Cosma, A. Marmier, C. Ramseyer, and C. Girardet, Phys. Rev. Lett. **78**, 1504 (1997).

[19] D. Ferry and J. Suzanne, Surf. Sci. **345**, L19 (1996).

[20] V. Panella, J. Suzanne, P. N. M. Hoang, and C. Girardet, J. Phys. I **4**, 905 (1994).

[21] D. L. Meixner, D. A. Arthur, and S. M. George, Surf. Sci. **261**, 141 (1992).

[22] M. Tarek, R. Kahn, and E. Cohen de Lara, Zeolites **15**, 67 (1995).

[23] J. A. C. Silva and A. E. Rodrigues, Ind. Eng. Chem. Res. **38**, 2434 (1999).

[24] F. Romá, J. L. Riccardo, and A. J. Ramirez-Pastor, Langmuir **21**, 2474 (2005).

[25] K. Binder and D. P. Landau, Surf. Sci. **108**, 503 (1981).

[26] W. Y. Ching, D. L. Huber, M. G. Lagally, and G.-C. Wang, Surf. Sci. **77**, 550 (1978); K. Kaski, W. Kinzel, and J. D. Gunton, Phys. Rev. B **27**, 6777 (1983); P. A. Rikvold, K. Kaski, J. D. Gunton, and M. C. Yalabik, *ibid.* **29**, 6285 (1984).

[27] R. Imbihl, R. J. Behm, K. Christmann, G. Ertl, and T. Matsushima, Surf. Sci. **117**, 257 (1982).

[28] B. Grosdidier, S. M. Osman, and A. Ben Abdellah, Phys. Rev. B **78**, 024205 (2008).

[29] M. C. Giménez and E. P. M. Leiva, Langmuir **19**, 10538 (2003).

[30] M. I. Rojas, M. C. Giménez, and E. P. M. Leiva, Surf. Sci. Lett. **581**, L109 (2005).

[31] M. C. Giménez and E. V. Albano, J. Phys. Chem. C **111**, 1809 (2007).

[32] M. C. Giménez, M. G.d el Pópolo, and E. P. M. Leiva, Electrochim. Acta **45**, 699 (1999).

[33] M. C. Giménez, M. G. del Pópolo, E. P. M. Leiva, S. G. García, D. R. Salinas, C. E. Mayer, and W. J. Lorenz, J. Electrochem. Soc. **149**, E109 (2002).

[34] M. C. Giménez, M. G. del Pópolo, and E. P. M. Leiva, Langmuir **18**, 9087 (2002).

[35] A. Milchev and M. Paunov, Surf. Sci. **108**, 25 (1981).

[36] A. Milchev, Electrochem. Acta **28**, 941 (1983).

[37] A. Milchev and K. Binder, Surf. Sci. **164**, 1 (1985).

[38] A. Milchev, J. Chem. Phys. **78**, 1994 (1983).

[39] O. A. Pinto, A. J. Ramirez-Pastor, and F. Nieto, Surf. Sci. **602**, 1763 (2008).

[40] O. A. Pinto, A. J. Ramirez-Pastor, and F. Nieto, Physica A **389**, 3456 (2010).

[41] O. A. Pinto, P. M. Pasinetti, F. Nieto, and A. J. Ramirez-Pastor, J. Chem. Phys. **134**, 064702 (2011).

[42] A. J. Ramirez-Pastor, T. P. Eggarter, V. D. Pereyra, and J. L. Riccardo, Phys. Rev. B **59**, 11027 (1999).

[43] M. Dávila, F. Romá, J. L. Riccardo, and A. J. Ramirez-Pastor, Surf. Sci. **600**, 2011 (2006).

[44] A. J. Ramirez-Pastor, M. S. Nazzarro, J. L. Riccardo, and G. Zgrablich, Surf. Sci. **341**, 249 (1995); A. J. Ramirez-Pastor, V. D. Pereyra, and J. L. Riccardo, Langmuir **15**, 5707 (1999); A. J. Ramirez-Pastor, J. L. Riccardo, and V. D. Pereyra, *ibid.* **16**, 682 (2000).

[45] N. Metropolis, A. W. Rosenbluth, M. N. Rosenbluth, A. H. Teller, and E. Teller, J. Chem. Phys. **21**, 1087 (1953).

[46] D. Nicholson and N. D. Parsonage, *Computer Simulation and the Statistical Mechanics of Adsorption* (Academic, London, 1982).

[47] V. A. Bakaev and W. A. Steele, Langmuir **9**, 148 (1992).

[48] A. J. Ramirez-Pastor and F. Bulnes, Physica A **283**, 198 (2000).

[49] E. Ising, Z. Phys. **31**, 253 (1925).

[50] C. Domb, in *Phase Transitions and Critical Phenomena*, edited by C. Domb and M. S. Green, Vol. 3 (Academic, London, 1974), p. 1; M. E. Fisher, Rep. Prog. Phys. **30**, 731 (1967).

[51] L. Onsager, Phys. Rev. **65**, 117 (1944).

[52] H. Bethe, Proc. R. Soc. London, Ser. A **150**, 552 (1935).

[53] T. Nitta, M. Kuro-oka, and T. Katayama, J. Chem. Eng. Jpn. **17**, 45 (1984).

[54] P. J. Flory, *Principles of Polymer Chemistry* (Cornell University Press, Ithaca, NY, 1953).

[55] A. J. Ramirez-Pastor, J. L. Riccardo, and V. Pereyra, Langmuir **16**, 10167 (2000).

[56] F. Romá, A. J. Ramirez-Pastor, and J. L. Riccardo, Langmuir **19**, 6770 (2003).

[57] M. M. Calbi, S. M. Gatica, M. J. Bojan, G. Stan, and M. W. Cole, Rev. Mod. Phys. **73**, 857 (2001).

[58] M. M. Calbi and J. L. Riccardo, Phys. Rev. Lett. **94**, 246103 (2005).

[59] L. Chen and J. K. Johnson, Phys. Rev. Lett. **94**, 125701 (2005).

[60] J. V. Pearce, M. A. Adams, O. E. Vilches, M. R. Johnson, and H. R. Glyde, Phys. Rev. Lett. **95**, 185302 (2005).

[61] L. Heroux, V. Krungleviciute, M. M. Calbi, and A. D. Migone, J. Phys. Chem. B **110**, 1297 (2006).

[62] F. Rittner, B. Boddenberg, M. J. Bojan, and W. A. Steele, Langmuir **15**, 1456 (1999).

[63] L. J. Dunne, G. Manos, and Z. Du, Chem. Phys. Lett. **377**, 551 (2003).